Acta Cryst. (1995). B**51**, 402–410

Crystallography in Four and Five Dimensions as Applied to Multi-Sublattice (Composite) Structures

BY PHILIP COPPENS

Department of Chemistry, State University of New York at Buffalo, Buffalo, New York 14260-3000, *USA*

(*Received* 9 *October* 1994; *accepted* 6 *March* 1995)

Abstract

Composite structures, containing two or more sublattices in one crystal, are of importance in the search for new materials. They are classified in terms of the interlattice matrix relating the sublattices, and by the use of chemical criteria. The use of superspace to interpret the diffraction pattern and perform calculations on electronic structure and lattice energy is referred to. The composite low-dimensional conductors (BEDT-TTF)$Hg_{0.776}(SCN)_2$ and $(BEDT\text{-}TTF)_4Hg_{2.88}Br_8$ (BEDT-TTF = bisethylene dithiotetrathiafulvalene) are discussed as examples. Of particular interest are the interaction between the sublattices and the change of structure and properties as a function of temperature.

Introduction

The crystallography of small unit-cell crystals is an essential component in the search for materials with new and interesting properties, as illustrated by the structural studies on the many varieties of high T_c superconducting ceramic materials, and by new developments in the field of microporous materials such as zeolites and AlPO5 polymorphs. To quote Cheetham (1994): 'it has become strikingly apparent that the most interesting of these materials exhibit complex stoichiometries – even non-stoichiometries – and include several components'.

Solids with *composite structure* are of particular relevance in this context. They contain two or more sublattices in one crystal. The sublattices are generally incommensurate in at least one direction, which implies that they are nonstoichiometric, as the ratio of the unit-cell volumes will deviate from integer values. When the components carry a net charge, as is common, mixed valency occurs by necessity. Composite structures occur naturally in minerals, such as valleriite $[Mg_{0.68}Al_{0.32}(OH)_2]_{1.562}[Fe_{1.07}Cu_{0.93}S_2]$ (Evans & Allmann, 1968; Organova, Drits & Dmitrik, 1972, 1973), and in many multicomponent synthetic materials. Among the best known examples of the latter are tetrathiofulvalene iodine, $(TTF)_7I_{5-x}$ (Johnson & Watson, 1976), and mercury arsenic hexafluoride $Hg_{3-\delta}AsF_6$ (Brown *et al.*, 1974). Composite structures have been referred to by a number of names, including misfit structures, intergrowth structures, chimney ladder structures and Vernier structures.

The number of known composite solids has increased rapidly in the past decade, although only very few cases with more than two sublattices are known. Since the sublattices interact through bonded and nonbonded interactions, distortions with the periodicity of the neighboring sublattice are introduced in each of the lattices. The sublattices are therefore modulated to an extent determined by the strength of the interactions. This adds additional complexity to these already unusual materials.

Direct space classification of composite crystals

The coexistence of two translational lattices in one body imposes a number of conditions if overlap is to be prevented. For two periodic objects to coexist in one crystal, *space fitting requirements* must be obeyed.

The relation between two direct space lattices of a composite crystal structure may be described by the equation

$$\mathbf{A}_2 = \sigma\mathbf{A}_1, \tag{1}$$

where σ is a (3×3) interlattice matrix relating the direct space translations of the sublattices. The corresponding reciprocal space relationship is given by

$$\mathbf{A}_2^* = (\sigma^{-1})^T\mathbf{A}_1^* = \sigma^*\mathbf{A}_1^*. \tag{2}$$

A composite crystal may consist of two different types of columnar structures with parallel but unequal repeat periods along the column axis. We will describe such structures as *columnar composite structures*. The condition that the columns be parallel restricts the *interlattice matrix* σ to the following form

$$\sigma = \begin{bmatrix} \sigma_{11} & \sigma_{12} & \sigma_{13} \\ \sigma_{21} & \sigma_{22} & \sigma_{23} \\ 0 & 0 & \sigma_{33} \end{bmatrix}, \tag{3}$$

where $\mathbf{c}$ is taken as the common column direction. The columns must fit together into an infinite array in the plane perpendicular to the column axis. This does not imply, however, that the $\mathbf{a}_1$ and $\mathbf{b}_1$ axes must be parallel to $\mathbf{a}_2$ and $\mathbf{b}_2$. The $\mathbf{a}_2$ axis may be in the plane defined by

$\mathbf{a}_1$ and $\mathbf{c}_1$, and $\mathbf{b}_2$ in the plane of $\mathbf{b}_1$ and $\mathbf{c}_1$, illustrated in Fig. 1(*a*). The direct space interlattice matrix is then given by

$$\sigma = \begin{bmatrix} \sigma_{11} & 0 & \sigma_{13} \\ 0 & \sigma_{22} & \sigma_{23} \\ 0 & 0 & \sigma_{33} \end{bmatrix}. \quad (4)$$

To avoid overlap of the two types of columns, the diagonal elements σ_{11} and σ_{22} must be integers or integer fractions. It follows that the direct space description of columnar composite structures requires *five* basis vectors in the three-dimensional space of the crystal.

Using (3), the reciprocal space relationship for columnar composite structures is obtained as

$$\mathbf{A}_2^* = \begin{bmatrix} 1/\sigma_{11} & 0 & 0 \\ 0 & 1/\sigma_{22} & 0 \\ -\sigma_{13}/(\sigma_{11}\sigma_{33}) & -\sigma_{23}/\sigma_{22}\sigma_{33} & 1/\sigma_{33} \end{bmatrix} \mathbf{A}_1^*, \quad (5)$$

which implies that the $\mathbf{a}^*$ and $\mathbf{b}^*$ axes of the two lattices are parallel. Thus, the two reciprocal lattices have the $hk0$ plane in common. The $\mathbf{a}^*$ and $\mathbf{b}^*$ axes are common when $\sigma_{11} = \sigma_{22} = 1$, as is usually the case. Expression (5) shows that columnar composite structures are described by *four* basis vectors in reciprocal space.

A second class of composite structures consists of stacked layers of different chemical composition. We will refer to this class, illustrated in Fig. 1(*b*), as *layer composite structures*. In this case the σ matrix is given by

$$\sigma = \begin{bmatrix} \sigma_{11} & \sigma_{12} & 0 \\ \sigma_{21} & \sigma_{22} & 0 \\ \sigma_{31} & \sigma_{32} & \sigma_{33} \end{bmatrix}, \quad (6)$$

where the in-plane axes have been labeled as **a** and **b**. Since the planes cannot overlap, the σ_{33} element is restricted to have an integer value by the space fitting requirement. Expression (6) implies the use of six basis vectors: $\mathbf{a}_1$, $\mathbf{b}_1$, $\mathbf{c}_1$ and $\mathbf{a}_2$, $\mathbf{b}_2$, $\mathbf{c}_2$. However, quite frequently the **a** and **b** axes of the two sublattices can be selected to be parallel, leading to

$$\sigma = \begin{bmatrix} \sigma_{11} & 0 & 0 \\ 0 & \sigma_{22} & 0 \\ \sigma_{31} & \sigma_{32} & n \end{bmatrix}, \quad (7)$$

in which n is an integer. When (7) applies, a *four*-basis-vector direct space description suffices.

Since $\mathbf{c}_1$ and $\mathbf{c}_2$ are not parallel, $(\mathbf{a}^*)_1$, $(\mathbf{a}^*)_2$ and $(\mathbf{b}^*)_1$, $(\mathbf{b}^*)_2$ will not be parallel either, unlike in columnar composite structures. The reciprocal interlattice matrix is now given by

$$\sigma^* = \begin{bmatrix} 1/\sigma_{11} & 0 & -\sigma_{31}/n\sigma_{11} \\ 0 & 1/\sigma_{22} & -\sigma_{32}/n\sigma_{22} \\ 0 & 0 & 1/n \end{bmatrix}. \quad (8)$$

For layer composite structures, only the $\mathbf{c}^*$ axis is common to the two sublattices; there is in general no common reciprocal lattice plane, as is the case for columnar composite structures. The diffraction pattern is therefore described by five basis vectors, compared with four basis vectors for two-component column composite structures. In direct space, the reverse is true as (7) involves only four basis vectors, while the matrix (4) relates a total of five vectors.

Although we have distinguished layer and column composite structures according to the form of the interlattice matrix, examination of the matrices (4) and (7) shows that intermediate cases classifiable in either category will occur. The interlattice matrix may be a diagonal matrix, or may be reducible to a diagonal matrix through a simple transformation of one of the lattices. The case of $(Bi_{0.55}Sr_{3.85}Ca_{5.60})Cu_{17}O_{29}$ (Frost-Jensen *et al.*, 1993; see Kato, 1990, for a similar structure of different composition) is illustrated in Fig. 2. The interlattice matrix is diagonal; the flat CuO_2 'ladders' at $\frac{1}{4}$ and $\frac{3}{4}$ along the vertical direction of the diagram can be considered either as columns, or as forming sheets through sideways interactions between the individual ladders.

Even though the distinction on the basis of symmetry is not always clear, as demonstrated by the latter case, the nature of the chemical interactions within the sublattices may be unambiguous. The sublattices of the heavy-metal sulfide intergrowth stuctures, such as $(SnS)_{1.17}NbS_2$

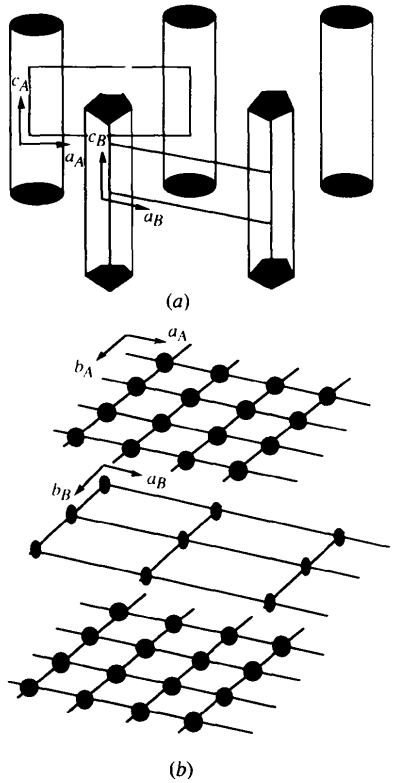

Fig. 1. Schematic illustration of the packing of the lattices in a composite structure. (*a*) Column composite structures, (*b*) layer composite structures.

(Wiegers *et al.*, 1989), are related to each other by a diagonal σ matrix. Nevertheless, the existence of layers within the structures makes the classification unambiguous. Such a *chemical classification* can include additional detail. Although a structure may be columnar on the basis of the symmetry classification, one component of the structure may form a strong three-dimensional lattice through covalent bonding, as in zeolites, or hydrogen bonding, as in urea inclusion complexes. In such *channel structures*, atoms or molecules forming the second lattice are positioned like 'guests' in the channels. In the urea host–guest inclusion complexes, long-chain hydrocarbons or substituted hydrocarbon molecules are included in channels within the hydrogen-bonded framework of urea molecules (Forst, Jagodzinsky, Boysen & Frey, 1987, 1990; Harris & Thomas, 1990; Harris, Smart & Hollingsworth, 1991). No composite examples of zeolite inclusion complexes appear to have been described at this time.

We note that the distinction between channel structures and columnar structures is not always clear-cut, as it depends on the nature of the interaction between the host molecules.

The occurrence of composite structures

While composite structures have for a long time been considered as oddities, they are not uncommon. They occur as minerals, and are often easily formed in the laboratory through 'self-assembly' of different components.

An early review of layer composite structures by Makovicky & Hyde (1981) lists a number of minerals with composite structures. Several of these, including koenenite and valleriite, have brucite-like layers consisting of Mg^{2+}, Al^{3+} and/or Fe^{3+} hydroxides with octahedral coordination of the metal atom and the general composition $M(OH)_2$. The hydroxide layers are interspersed with a NaCl-like layer of composition $[Na_4(Ca,Mg)_2Cl_{12}]^{4-}$ in the case of koenenite (Allmann, Lohse & Hellner, 1968), and a mixed sulfide layer of composition $[Fe_{1.07}Cu_{0.93}S_2]^{0.49-}$ in the case of valleriite (Evans & Allmann, 1968).

Layer composite structures, often referred to as intergrowth structures, occur in both natural and synthetic heavy metal sulfides. The composition $(MX)_xTX_2$ is common, as in $(LaS)_{1.14}NbS_2$ synthesized by Meerschaut, Rabu & Rouxel (1989) and analyzed by Wiegers, Meetsma, Haange, van Smaalen & de Boer (1990), and the mineral cylindrite $\approx FePb_3Sn_4Sb_2S_{14}$, in which layers alternate with respective compositions of $(Pb,Ag)_{14.3}Sn_{5.7}Sb_{4.4}Fe_{1.6}S_{26}$ and $Sn_{8.2}S_{2.3}Fe_{1.5}S_{24}$. The composition $(MX)_xTX_3$ occurs in the mineral cannizzarite with M and T representing both Pb and Bi, *i.e.* both layers contain Pb and Bi (Matzat, 1979). Other known inorganic examples are alloys such as $Re_{17}Ge_{22}$ (Jeitschko & Parthé, 1967) and 'infinitely adaptive' compounds of the type $Ba_p(Fe_2S_4)_q$, consisting of chains of edge-sharing Fe—S tetrahedra and columns of Ba ions (Swinnea & Steinfink, 1980).

Another large class of laboratory-prepared composite materials contains columns of iodine species such as I_3^- and I_5^- or higher homologs, embedded in a matrix of large organic or metallo-organic molecules (Coppens, 1982). The repeat period along the iodine columns is a function of the nature of the iodine species. A well studied example is tetrathiofulvalene iodine $(TTF)_7I_{5-x}$, analyzed by Johnson & Watson (1976). $TMA(TCNQ)_{2/3}I$ forms a commensurate composite structure in which the I_3^- repeat of 9.66 Å is 1.5 times the repeat in the TCNQ and TMA columns (Coppens *et al.*, 1980). In the diffraction pattern, the iodine layers are often diffuse along the layer direction, indicating a lack of correlation between the atomic positions in different columns. There is two-dimensional order in the lateral direction perpendicular to the columns, and one-dimensional order along the chains ('2+1' dimensional order), but not full three-dimensional order in the iodine sublattice. In $TMA(TCNQ)_{2/3}I$, the diffuseness of the layers, and therefore the degree of order, is a function of crystallization conditions and is probably also affected by varying the temperature of the sample.

The intercalated layer of graphite intercalation compounds may show long-range order along the layer direction, leading to multi-sublattice structures. Examples are $FeCl_3$-graphite (Cowley & Ibers, 1956), and $C_{64}Na$ in which eight graphite layers alternate with a

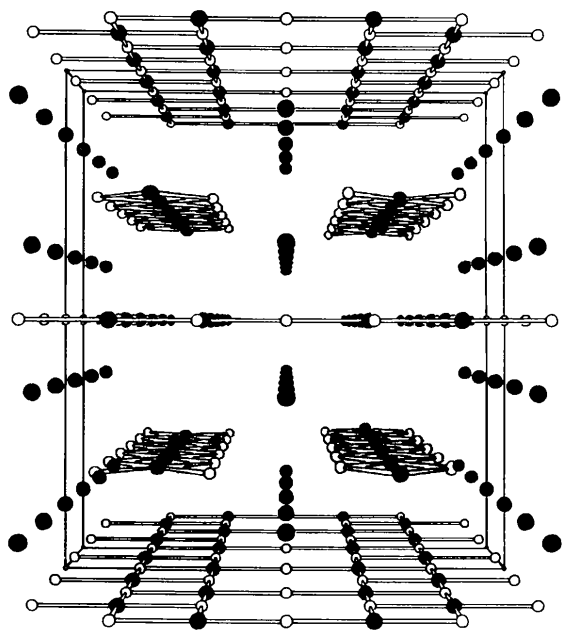

Fig. 2. The composite structure of $M_{10}Cu_{17}O_{29}$ viewed down the c axis. Filled circles are Cu atoms, O atoms are small open circles and M (Bi, Sr, Ca) are large filled circles. The CuO_2 ribbons at $\frac{1}{4}$, $\frac{3}{4}$ along the vertical axis of the diagram form the second sublattice (from Frost-Jensen *et al.*, 1993).

single Na layer (Asher, 1959). Many more such cases are likely to be found, especially when the temperature dependence of intercalation compounds is examined in more detail.

Composite structures are quite common among low-dimensional mineralo-organic conductors, often obtained by electrocrystallization. Some examples of this class discussed in the following section are (BEDT-TTF)$Hg_{0.776}(SCN)_2$ and (BEDT-TTF)$_4Hg_{3.89}Br_8$.

An example: the structure of (BEDT-TTF)$Hg_{0.776}(SCN)_2$

Crystals of (BEDT-TTF)$Hg_{0.776}(SCN)_2$ are grown by electrocrystallization (Wang *et al.*, 1991). The Hg atoms form the second sublattice, related to the first sublattice by the matrix

$$\sigma = \begin{bmatrix} 1.0 & -0.0077 & 0 \\ 0 & 1.2903 & 0 \\ 0 & 0.9083 & 1 \end{bmatrix}.$$

In this orientation, the **b** axis defines the incommensurate direction, and the $h0l$ reflections are common to both lattices. The projection down the incommensurate axis is shown in Fig. 3. The Hg atoms are coordinated by both ends of the SCN^- ions. However, because of the incommensurability of the two **b** axes, the coordination cannot be satisfied without the introduction of a distortion. This is clearly shown in the projection of the average structure (without the distortion), onto the *ab* plane, shown for the Hg and SCN entities in Fig. 4(*a*). The different periodicity of the Hg atoms and the SCN^- ions in the vertical dimension of the diagram is evident. The lack of commensurability between the repeats leads to a continuously varying coordination, including unacceptable distances as short as 1.90 Å for Hg—S. The interaction between the components of the two sublattices introduces a modulation in each (Fig. 4*b*), with a repeat equal to the periodicity of the second lattice. The modulative displacements are as large as 0.89 Å for the Hg atoms, while the SCN^- displacement waves have amplitudes of 0.16 Å and 12.1° for the translational and rotational waves, respectively.

The effect of the modulations on the Hg—S distances is shown in Fig. 5, in which the distances are plotted as a function of the four-dimensional coordinate t (de Wolff, 1977), which ensures that all the distances in the aperiodic crystal are represented. With the modulation (lower half of the figure) no anomalously short distances occur. When the bond valence sum (Brown & Altermatt, 1985) is evaluated for the Hg atom, it is found to be close to 2 when the modulation is included, but unrealistically large (because of the short distances) for the average structure without the modulation [Fig. 6 (Coppens, Cisarova, Bu & Sommer-Larsen, 1991)].

It is clear that the strong modulation in (BEDT-TTF)$Hg_{0.776}(SCN)_2$ is imposed by the unusual circumstances that the Hg atom is coordinated by S and N atoms in a lattice with different periodicity, so that the chemical bonding requirements can only be satisfied by large displacements of the coordinating atoms. The interaction between the two components in a column composite structure is illustrated in Fig. 7.

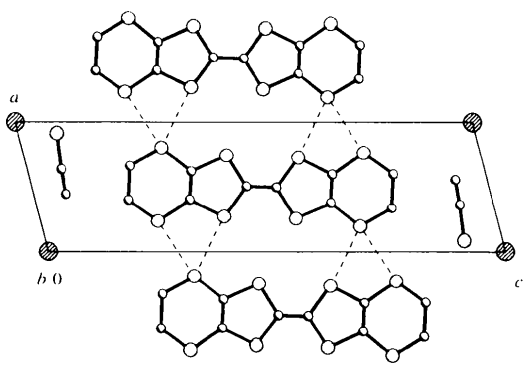

Fig. 3. The projection of the structure of (BEDT-TTF)$Hg_{0.776}(SCN)_2$ down the common *b* axis direction (from Wang *et al.*, 1991).

The diffraction pattern of composite crystals and the introduction of superspace

As each of the sublattices of an incommensurate composite crystal is incommensurately modulated with

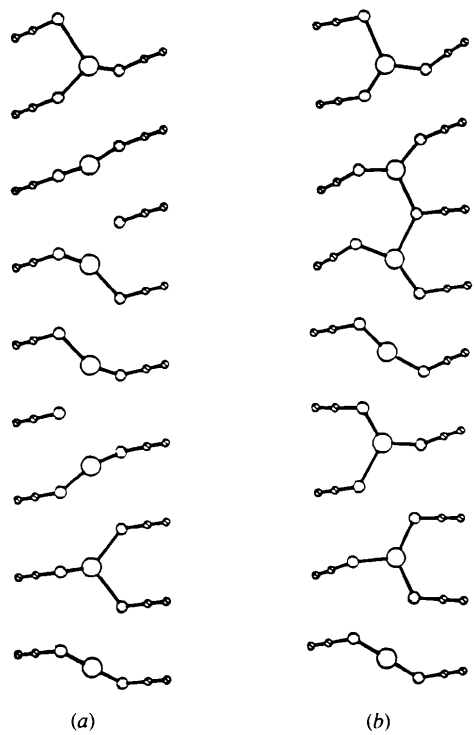

Fig. 4. The coordination of Hg and SCN in (BEDT-TTF)$Hg_{0.776}(SCN)_2$ projected on the *ab* plane. The **b** axis is the incommensurate axis. (*a*) Without the modulation; (*b*) with the modulation (from Wang *et al.*, 1991).

the periodicity of the adjacent sublattice, satellite reflections will occur. The diffraction pattern of a composite crystal is the superposition of the diffraction patterns of the two sublattices, *plus* satellite reflections representing the modulations (Janner & Janssen, 1980; van Smaalen, 1989).

As an example we will discuss the case represented by (5). The main reflections of the two sublattices have the indices *hkl*0, and *hk*0*m*, respectively, the reciprocal plane *hk*00 being common 'main–main' reflections. Reflections *hklm* with all nonzero indices occur because the modulation in sublattice *A* has the periodicity of the incommensurate repeat of sublattice *B* and *vice versa*. These '*pure*' *satellite reflections* are at the same time

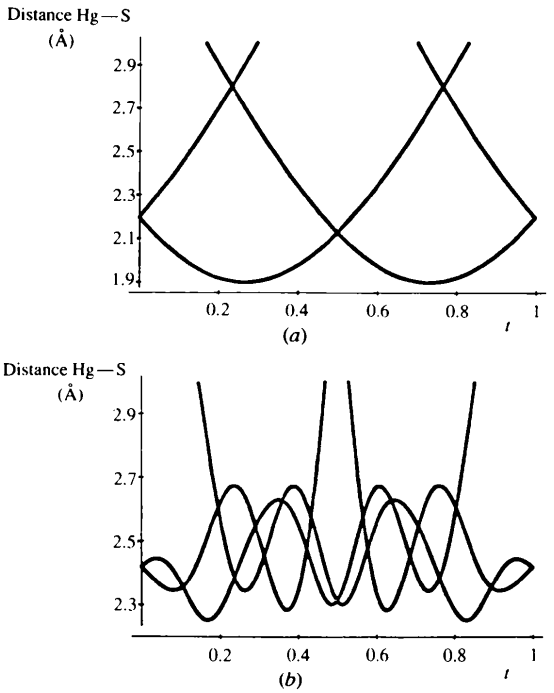

Fig. 5. Hg—S distances as a function of the four-dimensional coordinate *t*. (*a*) For the average structure, (*b*) including the modulation (from Coppens, Cisarova, Bu & Sommer-Larsen, 1991).

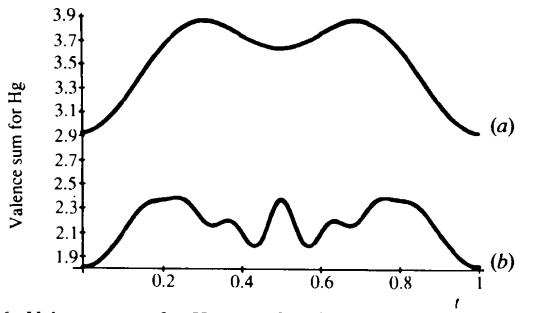

Fig. 6. Valence sums for Hg as a function of the four-dimensional coordinate *t*. (*a*) For the average structure, (*b*) for the true structure including the modulation (from Coppens, Cisarova, Bu & Sommer-Larsen, 1991).

*m*th-order satellites of sublattice *A*, and *l*th-order satellites of sublattice *B*. Using the same terminology, the *hkl*0 and *hk*0*m* reflections are *mixed main-satellite reflections*, as they are main reflections of one, and satellite reflections of the other sublattice.

de Wolff (1974) and Janner & Janssen (1977) realized that the periodicity, absent in at least one direction in the aperiodic crystal, can be retrieved by the use of superspace. It is schematically illustrated in Fig. 8, in which physical space is represented by the line $R3$, along which the two different periodicities can be observed. To retrieve the periodicity, the reflections are lifted out of the line $R3$ into the additional dimension. The main reflections of the second lattice lie along the axis $\mathbf{b}_4'$, which is obtained by adding the unit vector perpendicular to $R3$ to the reciprocal axis $\mathbf{b}_4$: $\mathbf{b}_4' = \mathbf{b}_4 + \mathbf{e}$. The satellite reflections, indicated by crosses, occupy the nonaxial grid points of the lattice.

The superdimensional direct space representation is obtained by using $\mathbf{a}_i'\mathbf{b}_j' = \delta_{ij}$, in which $\mathbf{a}_i'$ are the four-dimensional direct space axes. This means that at least one of the axes of a second sublattice is lifted out of three-dimensional space, as illustrated schematically in

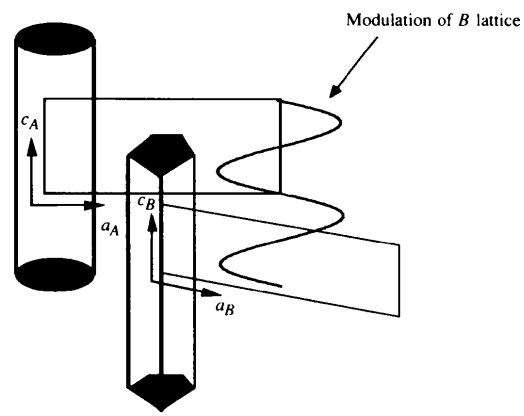

Fig. 7. Illustration of the interaction between the two components in a column composite structure. A distortion with period of sublattice *A* is introduced in sublattice *B*, and *vice versa*.

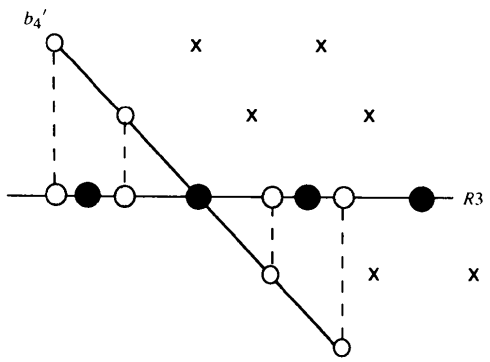

Fig. 8. The extra dimension in reciprocal space of a composite crystal. $R3$ represents three-dimensional space, with different periodicities of the two sets of reflections. Circles represent the main reflections of the two lattices; the crosses are satellite reflections.

Fig. 9. As in modulated structures, the atoms of the first sublattice become wavy strings along the extra dimension in superspace, with the amplitude of the wave corresponding to the modulative displacement. The atoms of the second sublattice are similar, but the strings in the fourth dimension are now in a direction parallel to one of the other direct axes of superspace, as illustrated in Fig. 9. The coordinate t, used in Figs. 5 and 6, varies from 0 to 1 in the direction perpendicular to $R3$. As it corresponds to a unit repeat in periodic superspace, it offers the means to represent all values of a property, such as an interatomic distance, anywhere in the aperiodic crystal in a single diagram.

Superspace group theory has been developed extensively (Janner & Janssen, 1977, 1979; de Wolff, Janssen & Janner, 1981; Janner, Janssen & de Wolff, 1983; van Smaalen, 1991; Janssen, Janner, Looijenga-Vos & de Wolff, 1992). Scattering factor expressions for composite structures can also be found in the literature (Coppens, Maly & Petricek, 1990; Yamamoto, 1993).

An interesting consequence of the nature of the diffraction pattern of composite structures is that information on the modulation of one sublattice can be obtained directly from a group of main-satellite reflections phased by the contribution of the main component. For (BEDT-TTF)$Hg_{0.776}(SCN)_2$ (b axis common and incommensurate), the Fourier map based on the $hkl0$ reflections is the projection of the four-dimensional structure down the b axis of the Hg lattice, which is the modulation vector of substructure (I) and a lattice translation of substructure (II). Thus, atoms of substructure (I) appear smeared out at their average positions, while those of substructure (II) show up as strings along $\mathbf{b}_1$ projected down the $\mathbf{b}_2$ axis, which is the b axis of the second substructure. This synthesis can be used to obtain the average position of the atoms of substructure (I) as an input model for a least-squares refinement, as well as to provide information on the modulation of the atoms of substructure (II). A section showing the Hg-atom string is reproduced in Fig. 10 (Cisarova, Maly, Petricek & Coppens, 1993).

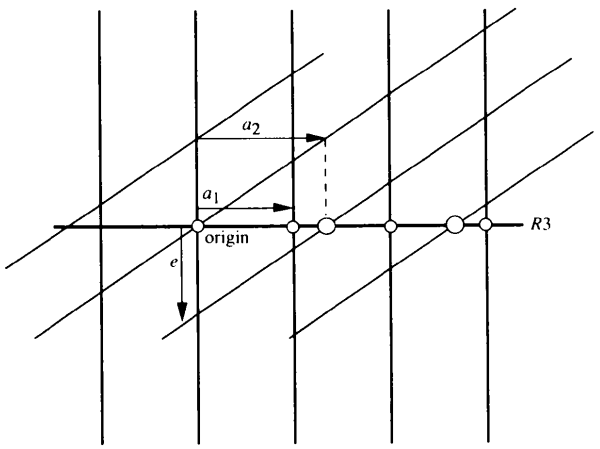

Fig. 9. Representation of a composite crystal in four-dimensional direct space. The horizontal line represents three-dimensional space, with two different periodicities indicated. The lines in the fourth dimension are strings representing the atoms of the two components without taking into account the modulation.

The temperature dependence of composite structures

The temperature dependence of composite structures is relatively unexplored. Unless vacancies develop, or a fraction of one component can separate from the crystals, as seems to be the case for the three-sublattice structure of $Hg_{2.86}AsF_6$ (Brown *et al.*, 1974), the volume contraction on cooling of coexisting sublattices must be the same. This condition is quite well fulfilled for (BEDT-TTF)$Hg_{0.776}(SCN)_2$, as shown in Fig. 11. The temperature dependence of the reflection intensities of (BEDT-TTF)$Hg_{0.776}(SCN)_2$ gives evidence for an additional *phonon temperature factor* for the Hg sublattice (Pressprich, van Beek & Coppens, 1994), which reflects a fluctuation of the phase of the modulation wave (Overhauser, 1971; Axe, 1980).

The two-component structure (BEDT-TTF)$_4Hg_{2.88}Br_8$ has, at room temperature, two polymorphic modifications both grown electrochemically, but under slightly different conditions (Li, Koster & Coppens, unpublished results). The different packing in the two phases is illustrated in Fig. 12. There are indications that the Hg lattice in the orthorhombic phase undergoes a transition below 100 K, while the monoclinic room-temperature Hg lattice of the monoclinic modification becomes triclinic slightly below room temperature, with unit-cell angles increasingly deviating from 90° as the temperature is lowered (Table 1; Li, 1994). This phase transition affects the relative position of the two components, while the structure of each appears mostly unchanged. It is interesting that the material becomes superconducting on further cooling to 4.2 K (Williams *et al.*, 1992; Lee, Naughton, Koster & Coppens, unpublished results).

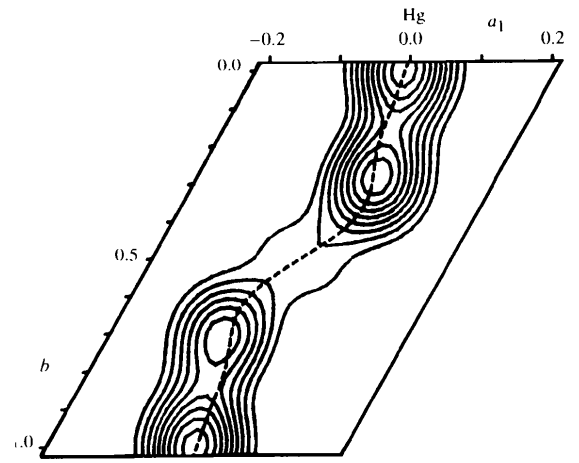

Fig. 10. $hkl0$ Fourier section of (BEDT-TTF)$Hg_{0.776}(SCN)_2$ containing the Hg atom. The **a** axis is horizontal; the **b** axis, which is the fourth axis for the Hg lattice, is inclined (from Cisarova, Maly, Petricek & Coppens, 1993).

The two polymorphs of (BEDT-TTF)$_4$Hg$_{2.88}$Br$_8$ appear to be the first composite structures for which phase transitions have been reported. However, phase transitions should be quite common as contraction on cooling will increase the interaction between the component lattices. In the low-dimensional composite structure of (5,10-diethylphenazinium)$_2$I$_{1.6}$, for example, the disorder in the iodine columns is reduced by cooling

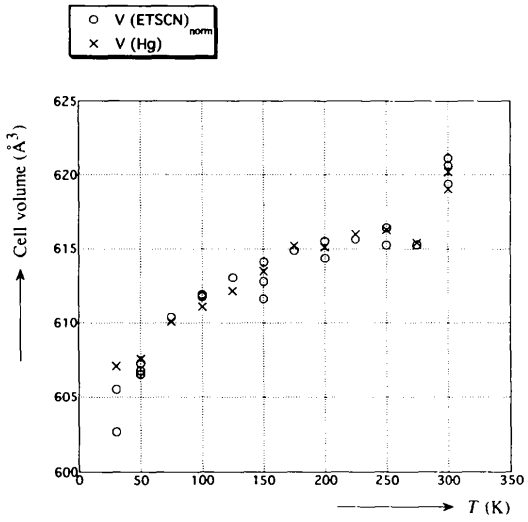

Fig. 11. Cell volumes for the two sublattices in (BEDT-TTF)Hg$_{0.776}$(SCN)$_2$ as a function of temperature. For the comparison, the volume of the (BEDT-TTF SCN) lattice has been normalized to the same average value as that of the Hg lattice (based on data from Pressprich, van Beek & Coppens, 1994).

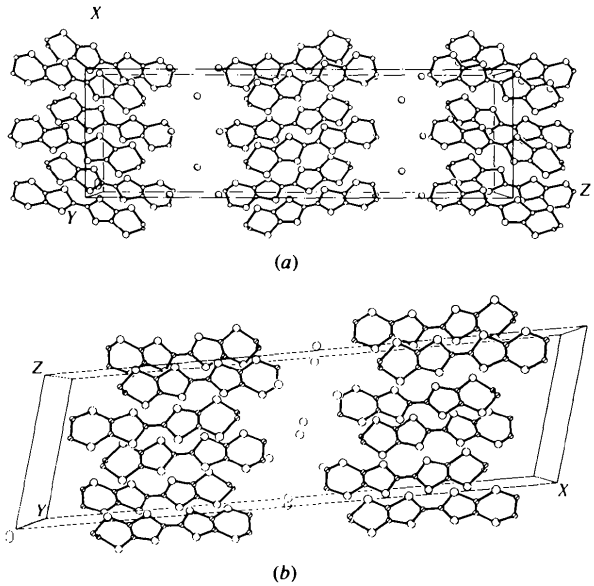

Fig. 12. Packing diagrams of the structures of (BEDT-TTF)$_4$Hg$_{2.88}$Br$_8$ viewed down the *b* axis. The Hg atoms which form the second sublattice, and are located at $z = \frac{1}{4}, \frac{3}{4}$ in both structures, are not shown. Large open circles: Br atoms; small open circles: S atoms. (*a*) Orthorhombic phase; (*b*) monoclinic phase (Li, 1994).

Table 1. (BEDT-TTF)$_4$Hg$_{2.88}$Br$_8$ *cell dimensions* (*Li*, 1994)

	Orthorhombic phase	Monoclinic phase	
	Room temperature	Room temperature	~70 K
Hg cell			
a (Å)	37.26 (5)	37.543 (4)	37.95 (4)
b (Å)	8.719 (2)	8.717 (1)	8.80 (1)
c (Å)	3.872 (4)	3.893 (1)	3.858 (5)
α (°)		—	96.73 (5)
β (°)		81.39 (1)	79.064 (8)
γ (°)		—	91.257 (2)
V (Å^3)	1258 (3)	1259.7 (4)	1256 (2)
BEDT-TTF cell			
a (Å)	37.21 (1)	38.610 (2)	38.64 (1)
b (Å)	8.718 (2)	8.717 (1)	8.629 (4)
c (Å)	11.273 (3)	11.223 (1)	11.011 (6)
α (°)	—	—	—
β (°)	—	74.058 (7)	74.70 (4)
γ (°)	—	—	—
V (Å^3)	3657 (2)	3631.4 (8)	3514 (2)
Volume ratio	2.91	2.88	2.86
Superspace group	*P*: *Pman*: $11\bar{1}(0,0,\gamma)$	*P*: *C*2/*c*: $\bar{1}1(0,0,\gamma)$	

while the modulation increases, as is evident from the 183–333 K diffraction study reported by Rosshirt, Frey, Boysen & Jagodzinsky (1985).

Calculation of the properties of composite structures

The calculation of the properties of composite structures requires the use of superspace. Sommer-Larsen & Gajhede (1991) have developed an approximate method for the calculation of the band structure of modulated structures in which the transfer integrals are developed as a Fourier series in the extra dimension. This method, when applied to the BEDT-TTF substructure of (BEDT-TTF)Hg$_{0.776}$(SCN)$_2$, shows that the modulation imposed in the composite structure creates a gap at the Fermi surface in certain regions of reciprocal space, and thereby prevents the nesting of the Fermi surface and a subsequent metal–insulator transition on cooling (Fig. 13). Not surprisingly, the density of state is also quite strongly affected by the modulation (Sommer-Larsen & Coppens, 1992, unpublished results).

The calculation of the lattice energy using pairwise atom–atom potentials can be modified to apply to modulated and composite structures, even though they are nonperiodic, using the superspace group description. To obtain the lattice energy, all pairwise interactions within each sublattice, and between sublattices, must be integrated over the four-dimensional coordinate. The composite crystal's lattice energy *W* is given by

$$W = \sum_{km} \sum_{ij} \int_0^1 e_{ij}[r_{ij}(t)]\mathrm{d}t,$$

where the sum *km* is over all sublattice combinations (including the 'self-interaction'), the sum *ij* is over all atom pairs in sublattices *k* and *m*, and e_{ij} is the pairwise interaction.

The integration over the fourth coordinate has been applied to the modulated structure of thiourea by Gao & Coppens (1989). For thiourea, the calculation correctly predicts an intermediate energy for the modulated phase, which occurs in the 169–202 K temperature interval between the paraelectric high-temperature and the ferroelectric low-temperature phases of thiourea. Similar calculations on composite structures are necessary to achieve an understanding of the phase transitions in these materials.

Concluding remarks

We conclude that the field of composite structures remains relatively unexplored. Although the symmetry classification is well understood, a relatively small number of composite crystals has been explored in detail, and little is known about the temperature dependence of many of the structures that have been studied. Given the ongoing search for complex new materials with interesting properties, the field is likely to grow considerably in coming years.

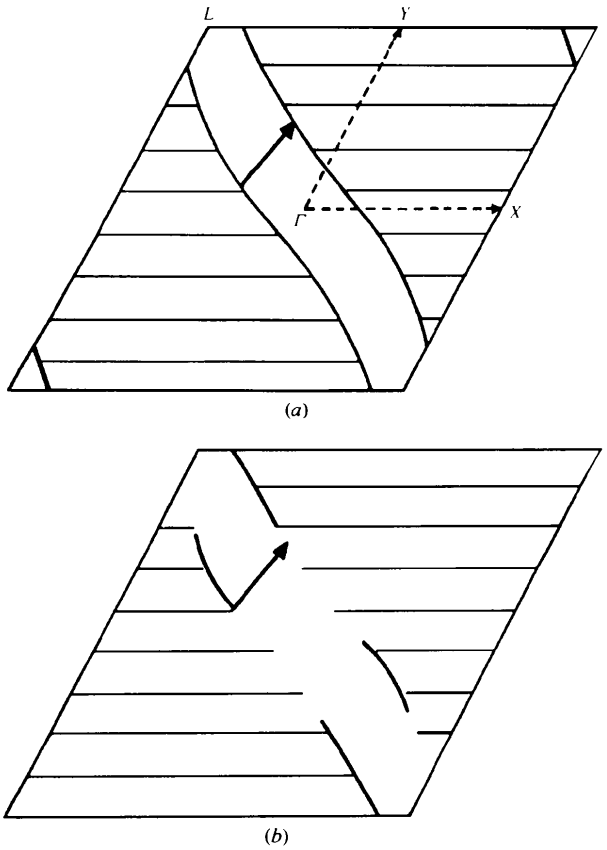

Fig. 13. Calculated Fermi surface for (BEDT-TTF)$Hg_{0.776}(SCN)_2$ in the a^*b^* plane. Hatched areas indicate regions where all levels are filled. $\Gamma = 0, 0; X = \pi a^*$, $Y = \pi b^*$. (*a*) Average structure, the nesting vector combining two sides of the Fermi surface is shown; (*b*) modulated structure. Part of the hatched regions now end up in a band gap, rather than on the Fermi surface. A nesting vector no longer reaching the other part of the Fermi surface is shown (from Sommer-Larsen & Coppens, 1992).

Part of the work reviewed here is based on PhD theses and publications of my coworkers X. Bu, I. Cisarova, A. Frost-Jensen, Y. Gao, G. Koster, R. Li, K. Maly, V. Petricek, M. R. Pressprich, P. Sommer-Larsen and C. van Beek, whose contributions are gratefully acknowledged. I would like to thank the National Science Foundation for financial support of this work (CHE9021069 and CHE9317770).

References

ALLMANN, R., LOHSE, H.-H. & HELLNER, E. (1968). *Z. Kristallogr.* **126**, 7–22.
ASHER, R. C. (1959). *J. Inorg. Nucl. Chem.* **10**, 238–249.
AXE, J. D. (1980). *Phys. Rev. B*, **21**, 4181–4190.
BROWN, I. D. & ALTERMATT, D. (1985). *Acta Cryst.* B**41**, 244–247.
BROWN, I. D., CUTFORTH, B. D., DAVIES, C. G., GILLESPIE, R. J., IRELAND, P. R. & VEKRIS, J. E. (1974). *Can. J. Chem.* **52**, 791–793.
CHEETHAM, A. K. (1994). *Science*, **264**, 794–795.
CISAROVA, I., MALY, K., PETRICEK, V. & COPPENS, P. (1993). *Acta Cryst.* A**49**, 336–341.
COPPENS, P. (1982). In *Extended Linear Chain Compounds*, edited by J. S. MILLER. New York: Plenum Press.
COPPENS, P., CISAROVA, I., BU, X. & SOMMER-LARSEN, P. (1991). *J. Am. Chem. Soc.* **113**, 5087–5089.
COPPENS, P., LEUNG, P., MURPHY, K. E., VAN TILBORG, P. R., EPSTEIN, A. J. & MILLER, J. S. (1980). *Mol. Cryst. Liq. Cryst.* **61**, 1–6.
COPPENS, P., MALY, K. & PETRICEK, V. (1990). *Mol. Cryst. Liq Cryst.* **181**, 81–90.
COWLEY, J. M. & IBERS, J. A. (1956). *Acta Cryst.* **9**, 421–431.
EVANS, H. T. JR & ALLMANN, R. (1968). *Z. Kristallogr.* **127**, 73–93.
FORST, R., JAGODZINSKY, H., BOYSEN, H. & FREY, F. (1987). *Acta Cryst.* B**34**, 187–189.
FORST, R., JAGODZINSKY, H., BOYSEN, H. & FREY, F. (1990). *Acta Cryst.* B**46**, 70–78.
FROST-JENSEN, A., LARSEN, F. K., JOHANNSEN, I., CISAROVA, I., MALY, K. & COPPENS, P. (1993). *Acta Chem. Scand.* **47**, 1179–1189.
GAO, Y. & COPPENS, P. (1989). *Acta Cryst.* B**45**, 298–303.
HARRIS, K. D. M. & THOMAS, J. M. (1990). *J. Chem. Soc. Faraday Trans.* **86**, 2985–2996.
HARRIS, K. D. M., SMART, S. P. & HOLLINGSWORTH, M. D. (1991). *J. Chem. Soc. Faraday Trans.* **87**, 3423–3431.
JANNER, A. & JANSSEN, T. (1977). *Phys. Rev. B*, **15**, 643–658.
JANNER, A. & JANSSEN, T. (1979). *Physica A*, **99**, 47–76.
JANNER, A. & JANSSEN, T. (1980). *Acta Cryst.* A**36**, 408–415.
JANNER, A., JANSSEN, T. & DE WOLFF, P. M. (1983). *Acta Cryst.* A**39**, 671–678.
JANSSEN, T., JANNER, A., LOOIJENGA-VOS, A. & DE WOLFF, P. M. (1992). *International Tables for Crystallography*, edited by A. J. C. WILSON, Vol. C, pp. 797–835, 843–844. Dordrecht: Kluwer Academic Publishers.
JEITSCHKO, W. & PARTHÉ, E. (1967). *Acta Cryst.* **22**, 417–430.
JOHNSON, C. K. & WATSON, C. R. (1976). *J. Chem. Phys.* **64**, 2271–2286.
KATO, K. (1990). *Acta Cryst.* B**46**, 39–44.
LEE, I. J., NAUGHTON, M. J., KOSTER, G. & COPPENS, P. Unpublished results.
LI, R. (1994). PhD Thesis. State University of New York at Buffalo.
LI, R., KOSTER, G. & COPPENS, P. Unpublished results.
MAKOVICKY, E. & HYDE, B. G. (1981). *Struct. Bonding*, **46**, 101–170.
MATZAT, E. (1979). *Acta Cryst.* B**35**, 133–136.
MEERSCHAUT, A., RABU, P. & ROUXEL, J. (1989). *J. Solid State Chem.* **78**, 35–45.
ORGANOVA, N. I., DRITS, V. A. & DMITRIK, V. A. (1972). *Kristallografiya*, **17**, 761–767.

ORGANOVA, N. I., DRITS, V. A. & DMITRIK, V. A. (1973). *Kristallografiya*, **18**, 966–977.
OVERHAUSER, A. W. (1971). *Phys. Rev. B*, **3**, 3173–3182.
PRESSPRICH, M. R., VAN BEEK, C. & COPPENS, P. (1994). *Acta Cryst.* A**50**, 461–467.
ROSSHIRT, E., FREY, F., BOYSEN, H. & JAGODZINSKY, H. (1985). *Acta Cryst.* B**41**, 66–76.
SMAALEN, S. VAN (1989). *J. Phys. Condens. Matter*, **1**, 2791–2800.
SMAALEN, S. VAN (1991). *Phys. Rev. B*, **43**, 11330–11341.
SOMMER-LARSEN, P. & COPPENS, P. (1992). Unpublished results.
SOMMER-LARSEN, P. & GAJHEDE, M. (1991). *Phys. Rev. B*, **43**, 5119–5131.
SWINNEA, J. S. & STEINFINK, H. (1980). *J. Chem. Ed.* **57**, 580–582.
WANG, H. H., BENO, M. A., CARLSON, K. D., THORUP, N., MURRAY, A., PORTER, L. C., WILLIAMS, J. M., MALY, K., BU, X., PETRICEK, V., CISAROVA, I., COPPENS, P., JUNG, D., WHANGBO, M.-H., SCHIRBER, J. E. & OVERMYER, D. L. (1991). *Chem. Mater.* **3**, 508–513.
WIEGERS, G. A., MEETSMA, A., HAANGE, R. J., VAN SMAALEN, S. & DE BOER, J. L. (1990). *Acta Cryst.* B**46**, 324–332.
WIEGERS, G. A., MEETSMA, A., VAN SMAALEN, S., HAANGE, R. J., WULFF, J., ZEINSTRA, T., DE BOER, J. L., KUYPERS, S., VAN TENDELOO, G., VAN LANDUYT, J., AMELINCKX, S., MEERSCHAUT, A., RABU, P. & ROUXEL, J. (1989). *Solid State Commun.* **70**, 409–413.
WILLIAMS, J. M., FERRARO, J. R., THORN, R. J., CARLSON, K. D., GEISER, U., WANG, H. H., KINI, A. M. & WHANGBO, M. H. (1992). *Organic Superconductors (Including Fullerenes): Synthesis, Structure, Properties, and Theory.* New Jersey: Prentice Hall.
WOLFF, P. M. DE (1974). *Acta Cryst.* A**30**, 777–785.
WOLFF, P. M. DE (1977). *Acta Cryst.* A**33**, 493–497.
WOLFF, P. M. DE, JANSSEN, T. & JANNER, A. (1981). *Acta Cryst.* A**37**, 625–636.
YAMAMOTO, A. (1993). *Acta Cryst.* A**46**, 831–846.